3-D FINITE ELEMENT MODELING OF THE REMOTE FIELD EDDY CURRENT EFFECT

Y. Sun and H. Lin

Department of Automatic Control
Nanjing Aeronautical Institute
Nanjing 210016
People's Republic of China

Y. K. Shin, Z. You, S. Nath and W. Lord

Department of Electrical Engineering and Computer Engineering
Iowa State University
Ames, Iowa 50011

INTRODUCTION

Differences between conventional single frequency eddy current (EC) nondestructive testing (NDT) and remote field eddy current (RFEC) NDT are summarized schematically in Fig. 1. In the testing of steam generator tubing, a differential probe (Fig. 1a) is used to produce impedance plane trajectories (Fig. 1c) which are indicative of the tubes condition. From a numerical simulation or modeling point of view, the finite element (FE) prediction of such impedance plane trajectories [1-3] requires a geometry of the dimensions shown in Fig. 1e. The relatively small mesh sizes associated with the FE simulation of EC probe behavior are a distinct advantage in that only modest computer resources are required. Indeed, for axisymmetric geometries, such code can run on a personal computer.

In the case of RFEC probes, however, the situation is vastly different. A typical RFEC probe [4,5] with exciter to sensor spacing of three pipe diameters is shown in Fig. 1b for the case of transmission gas-pipeline. The corresponding 'defect signal' (in this case the steady state AC phase difference between exciter and sensor coil signals) is shown in Fig. 1d and the required FE simulation geometry in Fig. 1f. The large area (for 2-D simulations) to be discretized in this case arises because of the exciter to sensor spacing and the need to eliminate tube edge effects from the defect signal [6]. This results in the need for extensive computer resources in order to simulate RFEC testing of transmission pipeline.

This comment is doubly valid in extending existing 3-D FE code [7] to RFEC geometries where one might be interested, for example, in simulating the RFEC probe response to a 10% through wall pit or very fine inter-granular stress corrosion cracking. The volumetric discretization required in this case represents a significant challenge even for today's best supercomputers. After describing the FE formulation, this paper discusses two aspects of the problem, namely node ordering and a "zoom-in" technique which shows promise for providing accurate simulation results for large pipeline geometries.

Review of Progress in Quantitative Nondestructive Evaluation, Vol. 9
Edited by D.O. Thompson and D.E. Chimenti
Plenum Press, New York, 1990

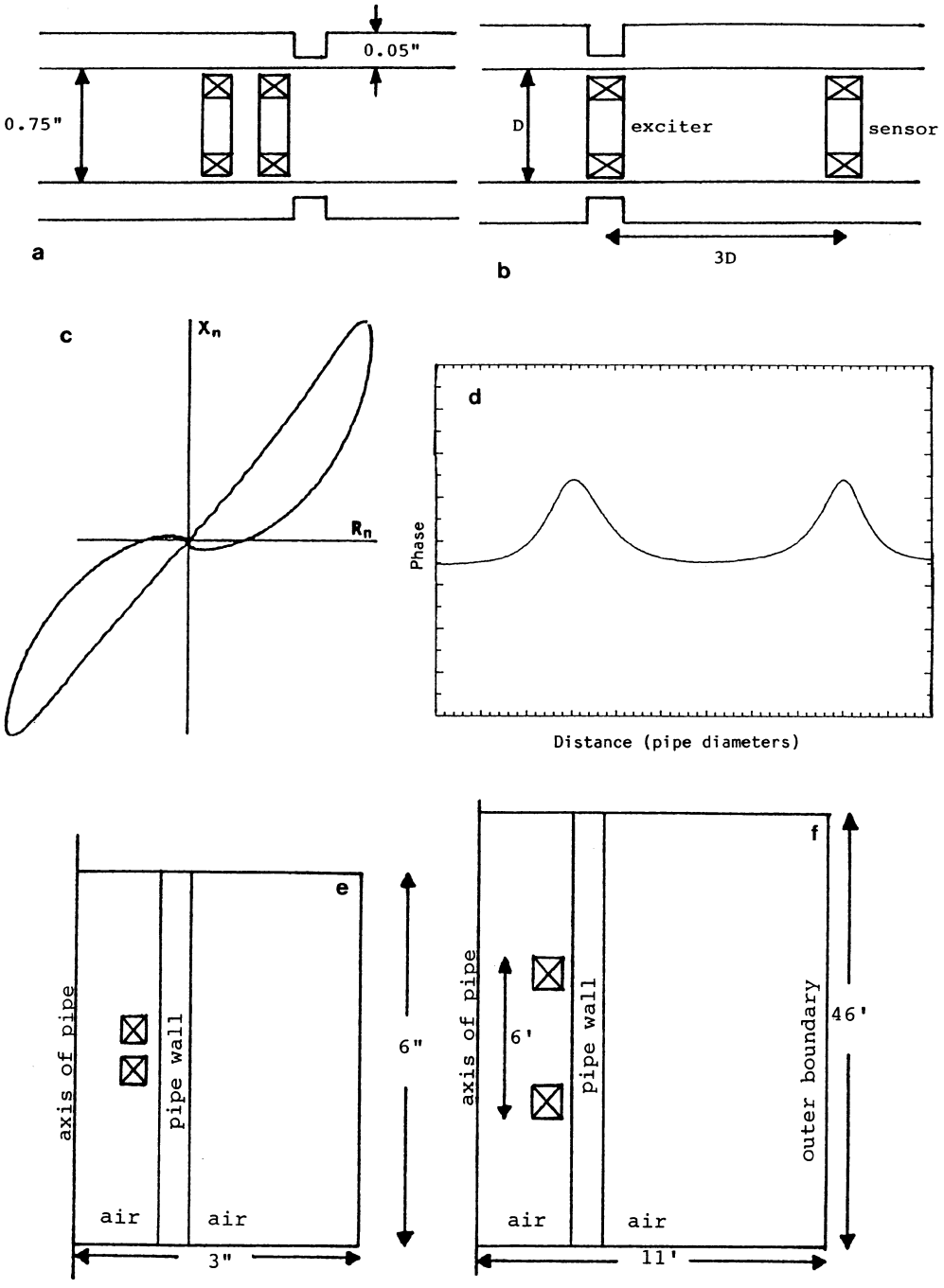

Fig. 1. Comparison of EC and RFEC modes of testing: (a) EC differential probe in a steam generator tube; (b) RFEC probe in a transmission gas-pipeline; (c) EC impedance plane trajectory for a tube O.D. defect; (d) RFEC phase difference plot for a pipe O.D. defect; (e) EC geometry needed for FE simulation; and (f) RFEC geometry needed for FE simulation.

FINITE ELEMENT FORMULATION

The partial differential equation governing RFEC phenomena is based on the principle of electromagnetic induction described by the Maxwell-Ampere law,

$$\oint_c \bar{H} \cdot d\bar{l} = \int\int_s \left(\bar{J} + \frac{\partial \bar{D}}{\partial t} \right) \cdot d\bar{S} \tag{1}$$

and the Maxwell-Faraday law,

$$\oint_c \bar{E} \cdot d\bar{l} = -\int\int_s \frac{\partial \bar{B}}{\partial t} \cdot d\bar{S} \tag{2}$$

In differential form these equations can be written as

$$\nabla \times \left(\frac{1}{\mu} \nabla \times \bar{A} \right) = \bar{J}_s - \sigma \frac{\partial \bar{A}}{\partial t} \tag{3}$$

where μ, $\bar{A}$, $\bar{J}_s$ and σ are the magnetic permeability (H/m), magnetic vector potential (Weber/m), applied current density vector in the coil (A/m^2), and the electrical conductivity (mhos/m), respectively. The quasi-static nature of the problem neglects displacement current. Assuming constant, single frequency operation and an isotropic material with no spatial variations in μ, Eq. (3) reduces to an elliptic PDE in terms of the phasor vectors $\hat{A}$ and $\hat{J}_s$,

$$\nu \nabla^2 \hat{A} = -\hat{J}_s + j\omega\sigma\hat{A} \tag{4}$$

where ν is the reluctivity (reciprocal permeability).

The finite element method does not give a direct analytical solution to this linear diffusion equation. Instead, the solution is obtained numerically by formulating an energy functional equivalent to the diffusion equation, discretizing the solution region by eight node hexahedral isoparametric elements, selecting an approximating function which ensures continuity across inter-element boundaries, and minimizing the energy functional with respect to each nodal value of potential. The resulting simultaneous algebraic equations are then solved to give the unknown magnetic vector potential values at each node in the region.

The three dimensional energy functional corresponding to the full 3-D Eq. (4) is

$$F(\hat{A}) = \int_v \left\{ \frac{1}{2}[\nu_x(\hat{A}_{zy} - \hat{A}_{yz})^2 + \nu_y(\hat{A}_{xz} - \hat{A}_{zx})^2 + \nu_z(\hat{A}_{yx} - \hat{A}_{xy})^2] \right.$$
$$\left. - (\hat{J}_x\hat{A}_x + \hat{J}_y\hat{A}_y + \hat{J}_z\hat{A}_z) + \frac{1}{2} j\omega\sigma(\hat{A}_x^2 + \hat{A}_y^2 + \hat{A}_z^2) \right\} dxdydz \tag{5}$$

where the first term represents the stored energy in the magnetic field, the second term represents the dissipated eddy current energy, and the third term is the input energy.

Functional minimization is achieved by substituting the approximating function,

$$\hat{A}(x,y,z) = \sum_i N_i(x',y',z')A_i \tag{6}$$

(where x', y' and z' are local coordinates) into the functional and setting its first derivative with respect to each of the unknown potentials to zero. That is,

$$\frac{\partial F(\hat{A})}{\partial A_{ki}} = 0 \qquad i = 1,2,3,\ldots,N; \qquad k = x,y,z \tag{7}$$

where N is the total number of nodes in the solution region. For convenience, instead of performing minimization node by node, it is performed element by element, and then the contribution of individual elements is summed to obtain 3N simultaneous linear algebraic equations which form a single global matrix equation,

$$[G]\{A\} = \{Q\} \tag{8}$$

where $[G]$ is the 3Nx3N banded nonsymmetric complex global matrix and $\{Q\}$ and $\{A\}$ are the 3Nx1 complex vectors of sources and unknowns, respectively. Eq. (8) can be solved by any standard solution technique such as Gauss elimination and the magnetic vector potential obtained. Other quantities such as flux density and induced emf can be calculated directly from the $\hat{A}$ values.

NUMERICAL STABILITY

As discussed in the introduction, the solution of 3-D RFEC problems is somewhat different from that of conventional EC problems because of the extremely low field intensity value in the RFEC remote field region. It has been found that an appropriate choice of the node numbering order is very important for numerical stability of the solution.

In general, the node numbering order does not affect the closed form solution of a matrix equation. However, in the case of numerical calucations, computer round-off errors may act as perturbation sources. For most electromagnetic field problems containing a ferromagnetic material, the difference in global matrix coefficient values is quite large because of the high permeability of the ferromagnetic material. Therefore, the solution of these problems is very sensitive to perturbations. Sharp changes of coefficient values in a matrix usually give rise to cancellation problems in the elimination process. Furthermore, the distribution of these sharp changes causes an accumulation of round-off errors which can result in perturbation sources in the numerical solution. The RFEC effect, characterized by far field quantities that are only about ten millionths of those in the near field region, may be entirely submerged in such errors if the perturbations are serious.

To avoid this kind of instability problem, it is necessary to group the coefficients of similar values as closely as possible by choosing a proper node numbering order which reduces the number of sharp changes in the global coefficient matrix. The 3-D node numbering order θ-Z-R appears to be the only proper choice among the three possible choices; Z-R-θ, θ-Z-R and R-θ-Z. Examples of the node numbering order Z-R-θ and θ-Z-R are shown in Fig. 2 and the corresponding matrix structures in Fig. 3. Figs. 4a and 4b show the steady state AC phase difference between exciter and sensor coil signals for each node numbering order when the exciter coil is fixed and the sensor coil is moved towards the remote field region. The result using the order Z-R-θ does not match the accurate axisymmetric result even for the denser discretization, while that using the order θ-Z-R shows good agreement.

"ZOOM-IN" TECHNIQUE

The need for extensive computer resources is one of the serious difficulties in applying the FE method to RFEC simulation in 3-D. An initial study [8] to overcome this difficulty has been made in an attempt to utilize the less demanding nature of the boundary element method. In certain cases, however, a special technique may be helpful from a practical point of view. Suppose the problem is

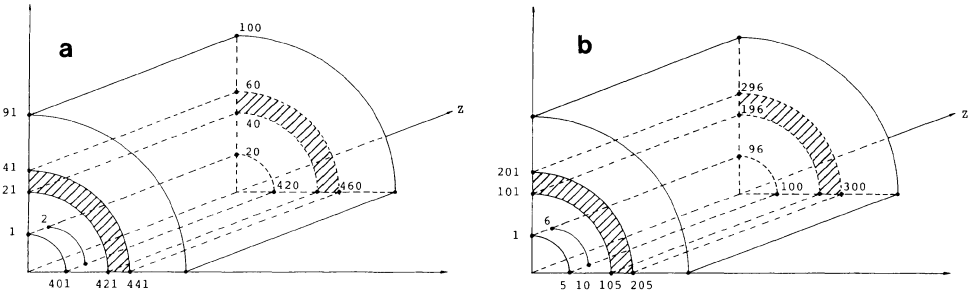

Fig. 2. Example of the node numbering order: (a) Z-R-θ and (b) θ-Z-R.

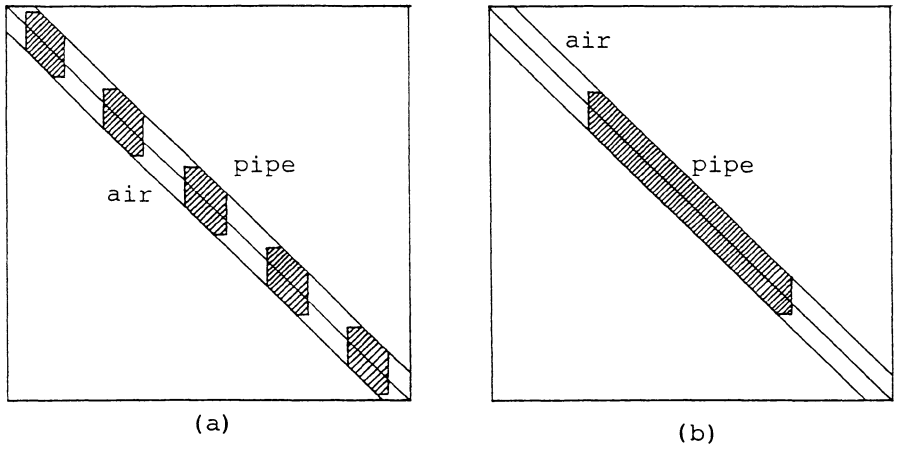

Fig. 3. Matrix structure: (a) Z-R-θ and (b) θ-Z-R.

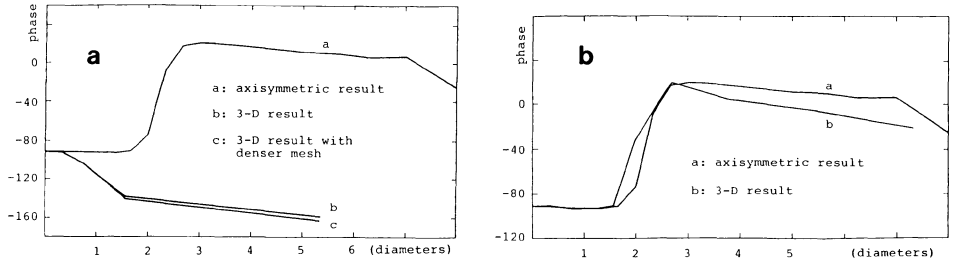

Fig. 4. FE Prediction of phase characteristics: (a) Z-R-θ and (b) θ-Z-R.

basically two dimensional or axisymmetric with the exception of a small local region such as the surface of a gas-pipeline having a fine inter-granular stress corrosion crack. If we make use of this 'almost 2-D' geometry in the calculation, computer resources can be reduced. This is the main idea behind the "zoom-in" technique.

Assume that the object to be modeled is a gas-pipeline having a small 3-D defect on the wall in the remote field region. Our interest is in the field changes around the defect. It is obvious that the area affected by the presence of the defect will be limited to a local region 'abcd' close to the defect (Fig. 5). The area outside the local region will not be affected much so that the solution for the outside area will almost be the same as that of the axisymmetric 2-D problem with or without a defect. Therefore, the local region can be treated as the full geometry for the 3-D solution, and the required boundary values of the local region can be found from the solution of the corresponding axisymmetric problem. To determine the location of the local region, proceed as follows:

1. Solve the axisymmetric problem without a defect.
2. Solve the same problem with an axisymmetric defect of the same dimensions as the real 3-D defect in R and Z directions.
3. Compare both solutions and select the smallest region where the difference of the two solutions is larger than the error to be allowed in the solution.

As the real 3-D defect is smaller than the axisymmetric defect, this procedure represents a conservative estimate of the local region.

Fig. 6 shows the relative steady state AC phase difference between exciter and sensor coil signals when the sensor coil passes the defect (in this case both coils move together) where an axisymmetric defect with a small pipe diameter was used to verify the validity of this technique.

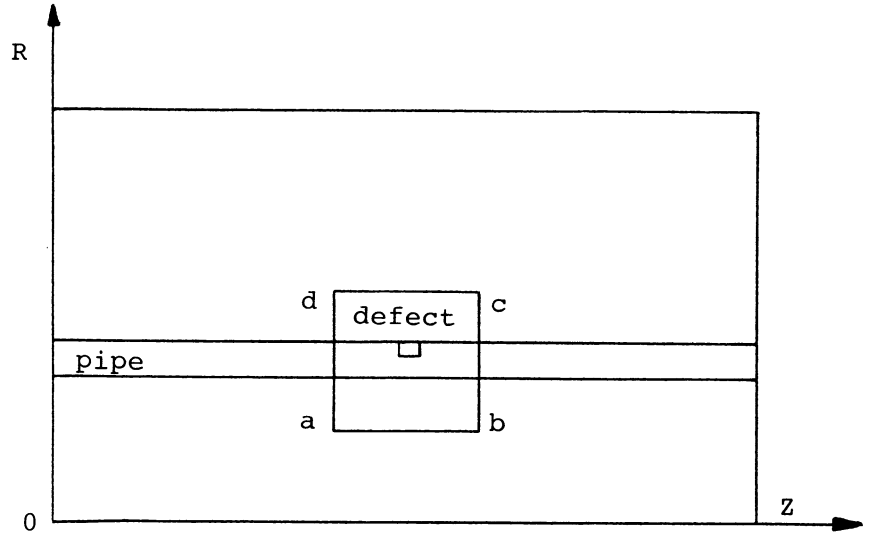

Fig. 5. Axisymmetric 2-D calculation region.

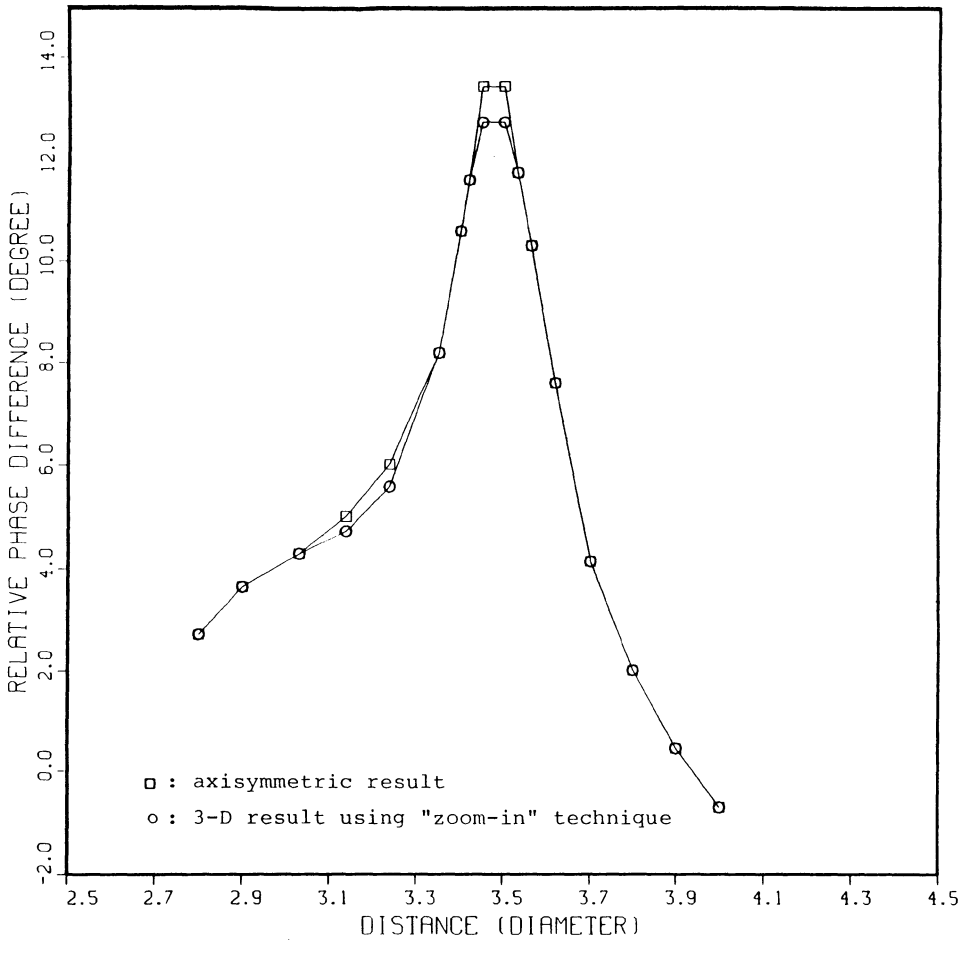

Fig. 6. FE Prediction of relative phase difference.

CONCLUSION

3-D FE modeling of RFEC phenomena appears to be feasible if adequate care is taken during node ordering and a "zoom-in" technique is used to limit the required computer resources. Additional work is needed on large diameter pipeline structures in order to validate these codes.

REFERENCES

1. R. Palanisamy and W. Lord, "Prediction of Eddy Current Probe Signal Trajectories." IEEE Transaction on Magnetics, Vol. 16, No. 5, p. 1083 (1980).

2. N. Ida, R. Palanisamy and W. Lord, "Eddy Current Probe Design Using Finite Element Analysis." Materials Evaluation, Vol. 41, No. 12, p. 1389 (1983).

3. N. Ida, H. Hoshikawa and W. Lord, "Finite Element Prediction of Differential EC Probe Signals from Fe_3P_4 Deposits in PWR Steam Generators," NDT International, Vol. 18, No. 6, p. 331 (1985).

4. T. R. Schmidt, "The Remote Field Eddy Current Inspection Technique," Materials Evaluation, Vol. 42, No. 2, p. 225 (1984).

5. W. Lord, Y. Sun, S. S. Udpa and S. Nath, "A Finite Element Study of the Remote Field Eddy Current Phenomenon," IEEE Transactions on Magnetics, Vol. 24, No. 1, p. 435 (1988).

6. S. Nath, M. S. Thesis, Colorado State University (1988).

7. N. Ida and W. Lord, "3-D Finite Element Modeling of Eddy Current NDT Phenomena," IEEE Transactions on Magnetics, Vol. 2, No. 6, p. 2635 (1985).

8. S. Nath, Y. K. Shin, T. J. Rudolphi and W. Lord, "Boundary Integral and Finite Element Simulation of Electromagnetic NDE Phenomena," these proceedings.